SLC4A7 suppresses lung adenocarcinoma oncogenesis by reducing lactate transport and protein lactylation

HAOJIE YAN[1-3*], QIAN HE[1,3,4*], YUBIAO GAO[1,3], XIAOMEI HE[1,3], HAITAO LUO[1-3], LIJUAN SHAO[1-3], JUN DONG[2] and FURONG LI[1,3,5]

[1]Translational Medicine Collaborative Innovation Center, Shenzhen People's Hospital (The Second Clinical Medical College of Jinan University; The First Affiliated Hospital, Southern University of Science and Technology), Shenzhen, Guangdong 518020, P.R. China; [2]Post-doctoral Scientific Research Station of Basic Medicine, Jinan University, Guangzhou, Guangdong 510632, P.R. China; [3]Guangdong Engineering Technology Research Center of Stem Cell and Cell Therapy, Shenzhen Key Laboratory of Stem Cell Research and Clinical Transformation, Shenzhen Immune Cell Therapy Public Service Platform, Shenzhen, Guangdong 518020, P.R. China; [4]School of Food and Drug, Shenzhen Polytechnic University, Shenzhen, Guangdong 518055, P.R. China; [5]Institute of Health Medicine, Southern University of Science and Technology, Shenzhen, Guangdong 518055, P.R. China

Received May 17, 2024; Accepted October 21, 2024

DOI: 10.3892/ijo.2025.5739

Abstract. Lactate and protein lactylation serve a key role in tumor pathogenesis. Solute carrier 4A7 (SLC4A7), a key transporter, participates in cellular acid homeostasis. However, its impact on lactate transport and protein lactylation in solid tumors, particularly lung adenocarcinoma (LUAD), remains largely unexplored. In the present study, lactylome analysis, Transwell and wound healing assay, animal experiments were conducted to validate functional regulation mediated by SLC4A7 in LUAD. SLC4A7 inhibited tumor progression, including metastasis, invasion and proliferation. Mechanistically, SLC4A7 decreased both intracellular and extracellular lactate accumulation and inhibited overall protein lactylation, as confirmed by lactylome analysis. Analyzing the lactylome revealed that SLC4A7 suppressed lysine lactylation of numerous genes like HSP90AA1 and pathways such as focal adhesion associated with carcinogenesis. Additionally, low expression levels of SLC4A7 in LUAD cancer stem cells were validated using tumor tissue samples from patients with LUAD. Moreover, the inhibitory role of SLC4A7 in regulating tumor stemness was verified. Collectively, the present results uncovered the inhibitory effect exerted by SLC4A7 on tumor progression via its regulation of lactate transport, protein lactylation and stemness properties. Targeting SLC4A7 may hold promise as a novel therapeutic strategy for LUAD.

Correspondence to: Professor Furong Li, Translational Medicine Collaborative Innovation Center, Shenzhen People's Hospital (The Second Clinical Medical College of Jinan University; The First Affiliated Hospital, Southern University of Science and Technology), 1017 Dongmen North Road, Luohu, Shenzhen, Guangdong 518020, P.R. China
E-mail: lifurong@mail.sustech.edu.cn

Professor Jun Dong, Post-doctoral Scientific Research Station of Basic Medicine, Jinan University, 601 Huangpu Avenue West, Guangzhou, Guangdong 510632, P.R. China
E-mail: dongjunbox@163.com

*Contributed equally

Key words: lung adenocarcinoma, lactate transport, protein lactylation, solute carrier 4A7

Introduction

Lung cancer is the second most common type of cancer, accounting for 12% of all cancer cases, and the leading cause of cancer-associated mortality worldwide (1). Therefore, development of more effective treatments for lung cancer is needed.

Lactate was initially considered a waste product of hypoxic glycolysis (2). However, in the 1920s, Otto Warburg observed that tumor cells consume more glucose and exhibit a preference for glycolysis over oxidative phosphorylation even in the presence of oxygen, resulting in elevated lactate production, a phenomenon known as the Warburg effect (3). Recent research has suggested that lactate serves a key role in tumor development (4,5). In addition to providing energy for tumor growth (6), lactate promotes tumor cell metastasis and invasion (7), regulates tumor angiogenesis (8,9), induces immunosuppression (10,11) and contributes to drug resistance (12,13). However, the molecular mechanism underlying lactate-mediated regulation of tumorigenesis remained largely unknown until the identification of lysine lactylation (Kla), a post-translational modification (PTM) of histones, in 2019 (14). Subsequent studies have demonstrated that histone lactylation promotes multiple key oncogenic processes such as reprogramming of immune cells and enhancement of cell plasticity (15,16). Recent studies have identified other proteins besides histones that undergo lactylation to modulate tumorigenesis (17-19). Cancer stem cells (CSCs) serve a key role in tumor metastasis, recurrence, immune evasion and drug resistance due to their capacity for renewal and tumorigenic

properties (20-23). Inhibiting lactate in CSCs may be a more effective therapeutic approach than bulk cells for various types of tumor (24-26). However, the regulatory mechanisms and factors of lactate and Kla in lung cancer remain largely unexplored.

Solute carrier (SLC) superfamily of membrane transporters on human cell membranes (including the inner membrane) comprises 65 subfamilies with >400 members (27,28). SLC transporters facilitate the transportation of a wide range of substrates across cellular membranes, including nutrients, metabolites and drugs (28,29). Due to their key role in cellular processes, numerous studies have demonstrated that these transporters serve an integral part in tumor development and may serve as promising therapeutic targets (30-32). Tumor metabolic reprogramming leads to excessive lactate production and contributes to a more acidic tumor microenvironment (TME) (33). Monocarboxylate transporter (MCT) 1 and 4 are highly expressed in various types of tumor and are responsible for transporting intracellular lactate to the TME to maintain intracellular pH homeostasis (34-37). Additionally, H^+-myo-inositol transporter SLC2A13 is a potential marker for CSCs in oral squamous cell carcinoma (38), suggesting an association between SLC transporters and CSCs. Apart from promoting tumor development, previous research has revealed that overexpression of SLC5A7, a member of the SLC5 family, is associated with favorable prognosis and enhances p53 protein expression to inhibit colorectal cancer progression (39). The bicarbonate transporter SLC4A7 is one of the Na^+-coupled HCO_3^- transporters involved in acid extrusion (40). SLC4A7 played a key role in the acidification of macrophage phagosomes (41). On the other hand, while accelerating breast carcinogenesis (42), SLC4A7 may serve a crucial role in suppressing tumor progression in prostate cancer (43). To the best of our knowledge, however, there is currently no research on the role of SLC4A7 in lung cancer or its association with lactate and CSCs.

The present study focused on lung adenocarcinoma (LUAD), which is the most prevalent subtype of lung cancer.

Materials and methods

Cell culture and reagents. Human non-small cell lung cancer cell lines H1975 and A549 were obtained from American Type Culture Collection. Quality control measures, including short tandem repeat identification and mycoplasma detection, were conducted to ensure authenticity of the cell lines. Cells were cultured in DMEM supplemented with 10% FBS (both Thermo Fisher Scientific, Inc.) at 37˚C under a 5% CO_2 atmosphere.

Tissue samples. Tumor tissues from two patients diagnosed with LUAD (two males, age, 51 and 43 years) were obtained from Shenzhen People's Hospital between June and September 2023 (Shenzhen, China), in accordance with the Declaration of Helsinki and as approved by the Ethics Committee of Shenzhen People's Hospital (approval no. 2023-065-01). All patients provided written informed consent.

Lentivirus infection. The lentiviruses utilized for overexpression and knockdown were obtained from GeneChem, Inc. For overexpression and knockdown of SLC4A7 (1 μg/μl), GV348 and GV493 were used respectively (both GeneChem, Inc). A549 and H1975 Cells ($5x10^5$) were seeded in a six-well plate and incubated at 37˚C for 24 h until 80% confluence. Lentivirus was mixed with transfection reagent A at MOI of 100 to cells according to the manufacturer's instructions for 24-48 h at 37˚C (GeneChem, Inc.). Puromycin (1 μg/ml) was added 72 h post-transfection to facilitate screening of stably infected cells and 2-3 days later for subsequent experiments (1 μg/ml puromycin used for maintenance). The target and control sequences of short hairpin RNA (shRNA) for SLC4A7 knockdown were 5'-GCAATGAAACTCTAGCACAAT-3' and 5'-TTCTCCGAACGTGTCACGT-3', respectively.

Reverse transcription-quantitative (RT-q)PCR. RT-qPCR was performed according to the manufacture's protocol as previously described (44). TRIzol (Thermo Fisher Scientific, Inc.) was employed for total RNA extraction from A549 and H1975 cells following the manufacturer's instructions. cDNA synthesis was performed according to the manufacturer's protocol using 1 μg total RNA and PrimerScript RT reagent kit (Takara Bio, Inc.). SYBR Green Master Mix (Takara Bio, Inc.) was used for RT-qPCR. Thermocycling conditions were as follows: Initial denaturation at 95˚C for 2 min. Denaturation at 94˚C for 15 sec, annealing and extension at 60˚C for 30 sec, 40 cycles. Relative mRNA expression was calculated using the $\Delta\Delta$Cq method (44) and GAPDH served as an internal control to normalize mRNA levels. The primer sequences were as follows: GAPDH forward, 5'-ACGGATTTGGTCGTATTGGG-3' and reverse, 5'-CGCTCCTGGAAGATGGTGAT-3'; SLC4A7 forward, 5'-CTTCTTATGATACACCATC-3' and reverse, 5'-GTTTACTCCATCGGTCAC-3'; SLC16A1 forward, 5'-TTGTTGGTGGCTGCTTGTCAGG-3' and reverse, 5'-TCATGGTCAGAGCTGGATTCAAG-3'; SLC16A3 forward, 5'-CCACAAGTTCTCCAGTGCCATTG-3' and reverse, 5'-CGCCAGGATGAACACGTACATG-3'; ALDH1A1 forward, 5'-CGGGAAAAGCAATCTGAAGAGGG-3' and reverse, 5'-GATGCGGCTATACAACACTGGC-3'; octamer-binding transcription factor 4 (OCT4) forward, 5'-GGGGTTCTATTTGGGAAGGTAT-3' and reverse, 5'-TACTGGTTCGCTTTCTCTTTCG-3'; SOX2 forward, 5'-ATGCACCGCTACGACGTG-3' and reverse, 5'-CTGGAGTGGGAGGAAGAG-3' and NANOG forward, 5'-ATAACCTTGGCTGCCGTCTC-3' and reverse, 5'-AGCCTCCCAATCCCAAACAA-3'.

Western blotting. Western blotting was performed as previously described (44). The harvested cells were lysed in a lysis buffer [50 mM Tris-HCl (pH 6.8), 2% sodium dodecyl sulfate, 1.5% DL-dithiothreitol, 10% glycerol and 0.2% Bromophenol blue] and lysed protein was quantified by bicinchoninic acid assay. A total of 20 μg/lane protein was subjected to SDS-PAGE using 4-20% gradient gel and transferred to Immobilon-FL PVDF. After blocking with 1X Protein Free Rapid Block Buffer (EpiZyme, PS108) at room temperature for 10 min, the membrane was incubated with the primary antibodies at 4˚C overnight. The antibodies were as follows: Anti-SLC4A7 (1:1,000; cat. no. ab82335; Abcam), anti-GAPDH (1:1,000; cat. no. 5174S; Cell Signaling Technology, Inc.), anti-Kla (1:1,000; cat. no. PTM-1401RM; PTM Biolabs Inc.), anti-ALDH1A1 (1:1,000; cat. no. 60171-1-Ig; Proteintech

Group, Inc.), anti-OCT4 (1:1,000; cat. no. 2750S; Cell Signaling Technology, Inc.), anti-SOX2 (1:1,000; cat. no. 2748S; Cell Signaling Technology, Inc.) and anti-NANOG (1:1,000; cat. no. ab109250; Abcam). The next day, the protein was washed with Tris-buffered saline +0.1% Tween-20 (TBST) three times and then incubated with secondary antibodies conjugated with horseradish peroxidase (HRP) (1:10,000; cat. no. 7074S; Cell Signaling Technology, Inc.) for 2 h at room temperature. Protein visualization was performed using ECL HRP substrate (34580, Thermo Fisher Scientific, Inc.) and achieved using a Syngene GeneGnome XRQ system (Syngene Europe) with auto-exposure mode. Exposure time was 20-120 sec to account for differential protein expression levels. The expression of protein was analyzed by ImageJ software (ImageJ 2.0; National Institutes of Health).

Transwell assay. Transwell assay was performed as previously described (44). DMEM 600 μl, Thermo Fisher Scientific, Inc.) containing 20% FBS (Thermo Fisher Scientific, Inc.) was added the bottom chamber of a Transwell plate. Subsequently, the upper chamber was loaded with 200 μl A549 or H1975 cell suspension with 1x10^5 cells. Following 24-h, 37˚C incubation period, cotton swabs were employed to remove the remaining cells on the inner side of the chamber. The migrated cells on the outer side were stained using a solution of 0.5% crystal violet at the room temperature for 20 min. After air-drying for 30 min at 80˚C, images of ≥5 random fields were captured utilizing an inverted light microscope. The migrated cells were quantified using ImageJ software (ImageJ 2.0; National Institutes of Health; three images/group). Next, the image was converted to black and white and the threshold was adjusted to contain all cells while removing impurities in the background. ImageJ enabled reliable automated cell counting via 'Analyze Particles' and manual confirmation of accuracy was conducted.

Wound healing assay. Each well of a six-well plate was seeded with ~1x10^6 A549 and H1975 cells and allowed to form monolayers (80-90% confluence) overnight. A sterilized pipette tip (20 μl) was used to create a straight line across the plate surface, followed by three washes with PBS to remove suspended cells. Images were captured at 0 h with a phase-contrast light microscope (magnification, x10x). Cells were cultured in DMEM supplemented with 2% FBS for 24 h at 37˚C under a 5% CO_2 atmosphere and images were obtained. Each assay was performed in triplicate. The scratch areas were quantified using ImageJ software. Briefly, the scratch area at day 0 was calculated and denoted by S_0; next, the area after 24 h (S_1) was calculated and the formula (S_0-S_1)/S_0 was used to calculate the migration.

Animal experiments. 16 BALB/c mice (16-17 g, female, age, 5-6 weeks) were obtained from GemPharmatech Co. Ltd. and housed in a specific pathogen-free environment (21-26˚C; humidity, 40-70%; light/dark cycle, 10 h:14 h; free access to food/water). A suspension of 5x10^6 H1975 cells in 200 μl PBS-Matrigel (1:1 ratio) was subcutaneously injected in the right underarm of mice. Nude mice were anesthetized by inhalation of isoflurane (induction, 5.0%; maintenance, 2.5%) prior to tumor cell injection. Tumor formation was monitored and weight of mice with tumors was measured twice/week. In strict accordance with animal ethical regulations, the weight of tumors did not exceed 10% of the mouse body weight, the average tumor diameter did not exceed 20 mm and the tumor volume did not exceed 2,000 mm^3. After 16 days, all animals were sacrificed by carbon dioxide asphyxiation prior to removing the tumor, maintaining a CO_2 replacement rate of 30-70% of the chamber volume/min. Death was confirmed 2 min after observation of cessation of movement and respiration and pupil dilation. All experimental protocols were approved by the Institutional Ethics Committee of Shenzhen People's Hospital (approval no. AUP-230220-YHJ-0085-01). All animal experiments were conducted following the guidelines set by the Institutional Ethics Committee of Shenzhen People's Hospital and all the methods employed were in accordance with the ARRIVE guidelines (44).

Measurement of lactate. Lactate was measured with a lactate kit (cat. no. LCSSH-0816W; Lunchangshuo Biotech) according to the manufacturer's instructions. Briefly, for extracellular lactate analysis, 1x10^6 A549 and H1975 cells were cultured in serum-free DMEM for 24 h at 37˚C. Subsequently, 1 ml culture medium was centrifuged at 4˚C, 12,000 g, 10 min to remove the supernatant. For intracellular lactate analysis, cells were cultured at 37˚C for 48-72 h in DMEM supplemented with 10% FBS and harvested (1x10^6 cells). Lysis buffer (200 μl) was added to release lactate from cells. Finally, the concentration of lactate in each sample was determined based on a standard curve created by colorimetry.

Protein extraction and digestion. Cells were supplemented with 4-fold volume of lysis buffer (8 M urea, 1% protease inhibitor, 3 μM trichostatin A and 50 mM nicotinamide) and subjected to sonication three times on ice using a high-intensity ultrasonic processor (Ningbo Scientz Biotechnology Co., Ltd.). The sonication cycle was set as follows: ultrasound 10 sec, pause 20 sec, repeat 3-5 times. Following centrifugation at 4˚C for 10 min at a speed of 12,000 x g, the supernatant was transferred to a new centrifuge tube and protein concentration was determined using BCA kit. For digestion, the protein solution was reduced with 5 mM dithiothreitol for 30 min at 56˚C and alkylated with 11 mM iodoacetamide for 15 min at room temperature in darkness. Subsequently, the protein was diluted with triethanolamine buffer to achieve a urea concentration <2 M. Finally, trypsin was added at a trypsin-to-protein mass ratio of 1:50 for overnight digestion at 37˚C followed by digestion of 4 h at a trypsin-to-protein mass ratio of 1:100 at 37˚C. The resulting peptides were then desalted using a C18 SPE column.

Pan-antibody-based PTM enrichment. Enrichment assay was performed according to a previously described protocol (18). To enrich Kla-modified peptides, tryptic peptides dissolved in NETN buffer (100 mM NaCl, 1 mM EDTA, 50 mM Tris-HCl, 0.5% NP-40, pH 8.0) were incubated with pre-washed antibody beads (cat. no. PTM-1404; PTM Biolabs Inc.) at 4˚C overnight with gentle shaking. Subsequently, beads were subjected to four washes with NETN buffer followed by two washes with H_2O. The bound peptides were eluted from beads using 0.1% trifluoroacetic acid and the eluted fractions were combined and vacuum dried. For liquid chromatography with

tandem mass spectrometry (LC-MS/MS) analysis, peptides were desalted using C18 ZipTips (MilliporeSigma) according to the manufacturer's instructions.

LC-MS/MS. LC-MS/MS analysis was performed as described previously (18). Briefly, peptides were dissolved in solvent A using LC and separated by a NanoElute ultra-high performance liquid phase system (6-22% B for 40 min, 22-30% B for 12 min, 30-80% B for 4 min and 80% B for 4 min). The separated peptides were injected into the capillary ion source for ionization and analyzed by timsTOF Pro 2 MS (Bruker), which was operated in parallel accumulation serial fragmentation mode.

MS/MS data were processed using MaxQuant search engine (v.1.6.15.0). Tandem mass spectra were searched against the human SwissProt database (20,422 entries) concatenated with a reverse decoy database. Trypsin/P was specified as cleavage enzyme, allowing ≤2 missing cleavages. The mass tolerance for precursor ions was 20 ppm in the first search and 5 ppm in the main search, while the mass tolerance for fragment ions was 0.02 Da. Carbamidomethyl on Cys was specified as fixed modification and acetylation on protein N-terminus and oxidation on Met were designated as variable modifications. The false discovery rate was adjusted to <1%.

ALDEFLUOR assay. Isolation of $ALDH^+$ cells was conducted using the ALDEFLUOR™ kit (cat. no. 01700; Stemcell Technologies, Inc.), as previously described (45). In brief, cells were treated with ALDEFLOUR assay buffer containing activated ALDEFLOUR™ Reagent BODIPY-aminoacetaldehyde and analyzed using a fluorescence-activated cell sorting instrument (Sony Group Corporation) and isolated $ALDH^{+/-}$ cells. Tumor tissue was dissociated into single-cell suspensions using Tumor Dissociation kit (cat. no. 130-095-929; Miltenyi Biotec GmbH) prior to sorting.

Colony formation assay. Colony formation assay was performed as previously described (45). Briefly, 5,000 cells/well were seeded in six-well tissue culture plates and cultured for 10 days. The cell monolayer was washed with PBS and fixed with 4% paraformaldehyde for 15 min. After removing the paraformaldehyde, each well was stained with 800 μl crystal violet staining solution for 15 min. The staining solution was discarded and the plates were washed with PBS until they became clear. Finally, the culture plates were air-dried at room temperature and the colonies were counted.

MTS assay. Cell proliferation was assessed by MTS assay (cat. no. KGA327; Nanjing KeyGen Biotech Co., Ltd.) in 96-well plates with a seeding density of 1,000 cells/well, following the manufacturer's instructions.

Statistical analysis. Statistical analyses were performed using R statistical environment (version 4.2.0; R Foundation for Statistical Computing). Data were analyzed by Student's t test or two-way ANOVA followed by post hoc Sidak's test. For enrichment analysis, proteins were classified by Gene Ontology (GO; geneontology.org/) annotation into three categories: Biological process, cellular compartment and molecular function. For each category, two-tailed Fisher's exact test was used to evaluate the enrichment of the differentially expressed protein against all identified proteins. $P<0.05$ was considered to indicate a statistically significant difference. Regarding enrichment of pathway analysis, Kyoto Encyclopedia of Genes and Genomes (KEGG; kegg.jp/) database was used to identify enriched pathways, assessed by two-tailed Fisher's exact test. Corrected $P<0.05$ was considered to indicate a statistically significant difference. Pathways were classified into hierarchical categories according to the KEGG website.

Results

SLC4A7 inhibits LUAD progression. To investigate the role of SLC4A7 in LUAD, stable cell lines with overexpression or knockdown of SLC4A7 were generated in A549 and H1975 cells. The expression of SLC4A7 was confirmed using RT-qPCR and western blotting (Fig. S1). Transwell and wound healing assays were conducted to assess the migratory and invasive effects regulated by SLC4A7. The overexpression of SLC4A7 significantly suppressed cell migration and invasion in both A549 and H1975 cell lines (Fig. 1A and B). Conversely, knockdown of SLC4A7 substantially enhanced the cell migratory and invasive abilities (Fig. 1C and D).

To validate its impact *in vivo*, equal numbers of H1975 cells overexpressing SLC4A7 or control cells were separately injected subcutaneously into BALB/c nude mice. SLC4A7 overexpression inhibited tumor growth and prevented tumor formation (Fig. 1E). Tumor weight and volumes were significantly lower in the group with overexpression of SLC4A7 compared with the control group (Fig. 1F and G), as well as change in tumor volume (Fig. S2A). No significant difference was observed in mouse weight throughout the experiment (Figs. 1H and S2B). Overall, the present study provided novel evidence of an inhibitory effect of SLC4A7 on LUAD progression.

SLC4A7 affects lactate transport by inhibiting SLC16A1/3 expression. To elucidate the regulatory mechanism of SLC4A7 in tumors, whether it also regulates lactate transport was investigated, as certain members of the SLC family are involved in this process (35). Cells were cultured in a serum-free medium for 24 h, and lactate concentration was measured. Overexpression of SLC4A7 significantly reduced lactate levels in both A549 and H1975 cell lines (Fig. 2A). Conversely, downregulation of SLC4A7 expression led to increased lactate accumulation in cell culture medium (Fig. 2B). These results highlighted the potential role of SLC4A7 in the TME due to its impact on lactate metabolism. To understand how SLC4A7 affects lactate accumulation, expression levels of SLC16A1 and SLC16A3 (35) (key transporters involved in lactate transportation within tumors) were examined. Overexpression of SLC4A7 resulted in decreased expression of both SLC16A1 and SLC16A3, while knockdown of SLC4A7 led to their upregulation (Fig. 2C-F). These findings suggested that inhibition of SLC16A1/3 expression may be a mechanism by which SLC47 regulates lactate transport.

SLC4A7 impairs protein lactylation. Given that protein lactylation, including lactylation of histone and non-histone proteins, is involved in tumor development, the potential

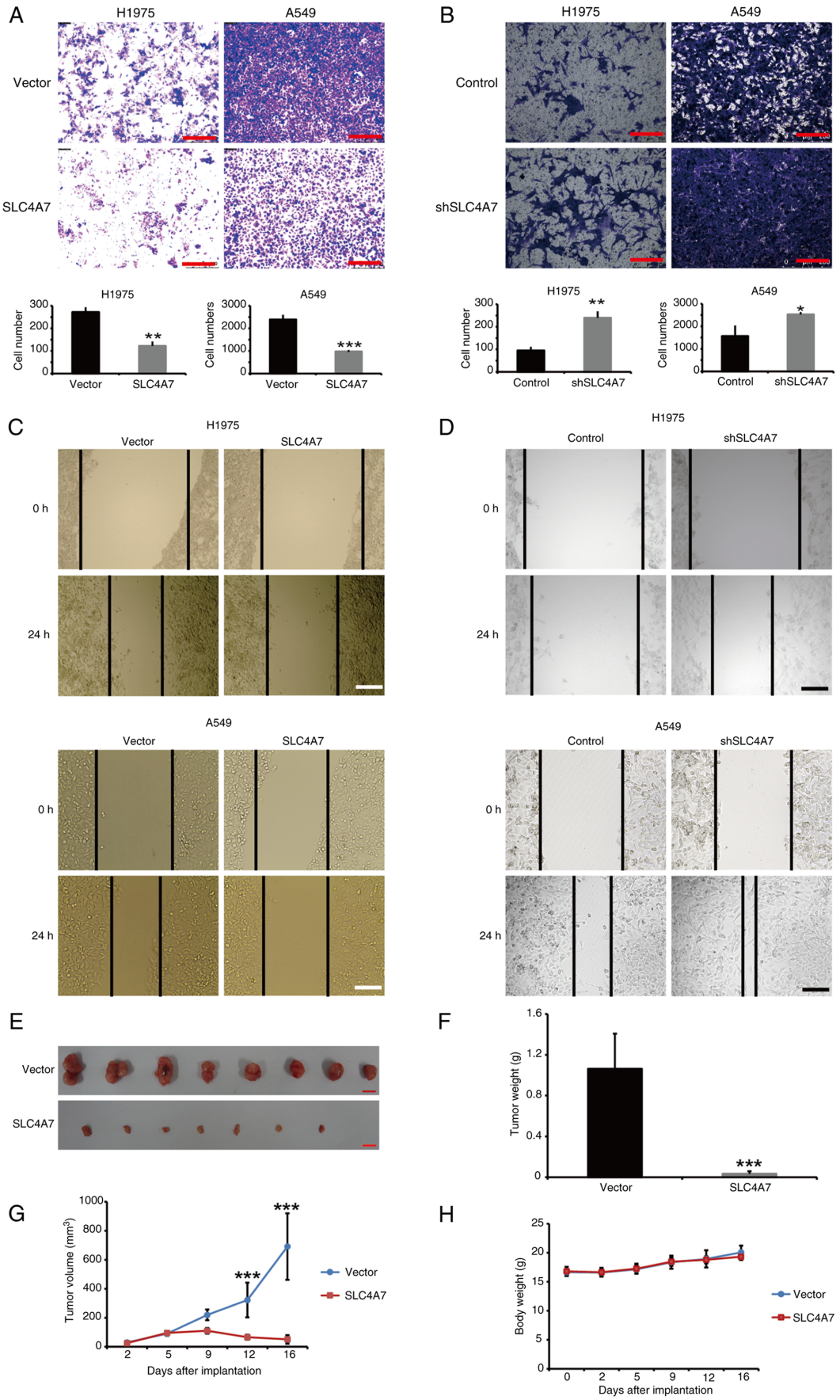

Figure 1. SLC4A7 suppresses lung adenocarcinoma development both *in vitro* and *in vivo*. Transwell assay in H1975 and A549 cell lines with SLC4A7 (A) overexpression and (B) knockdown. Scale bar, 250 μm. Wound healing assay in H1975 and A549 cell lines with SLC4A7 (C) overexpression and (D) knockdown. Scale bar, 150 μm. (E) Subcutaneous injection of $5x10^6$ cells into BALB/c nude mice resulted in tumor formation after 16 days (n=8/group). Scale bar, 1 cm. Tumor (F) weight and (G) volume. (H) Mouse body weight during the experiment (n=8). *P<0.05, **P<0.01, ***P<0.001 vs. vector/control. SLC4A7, solute carrier 4A7; sh, short hairpin.

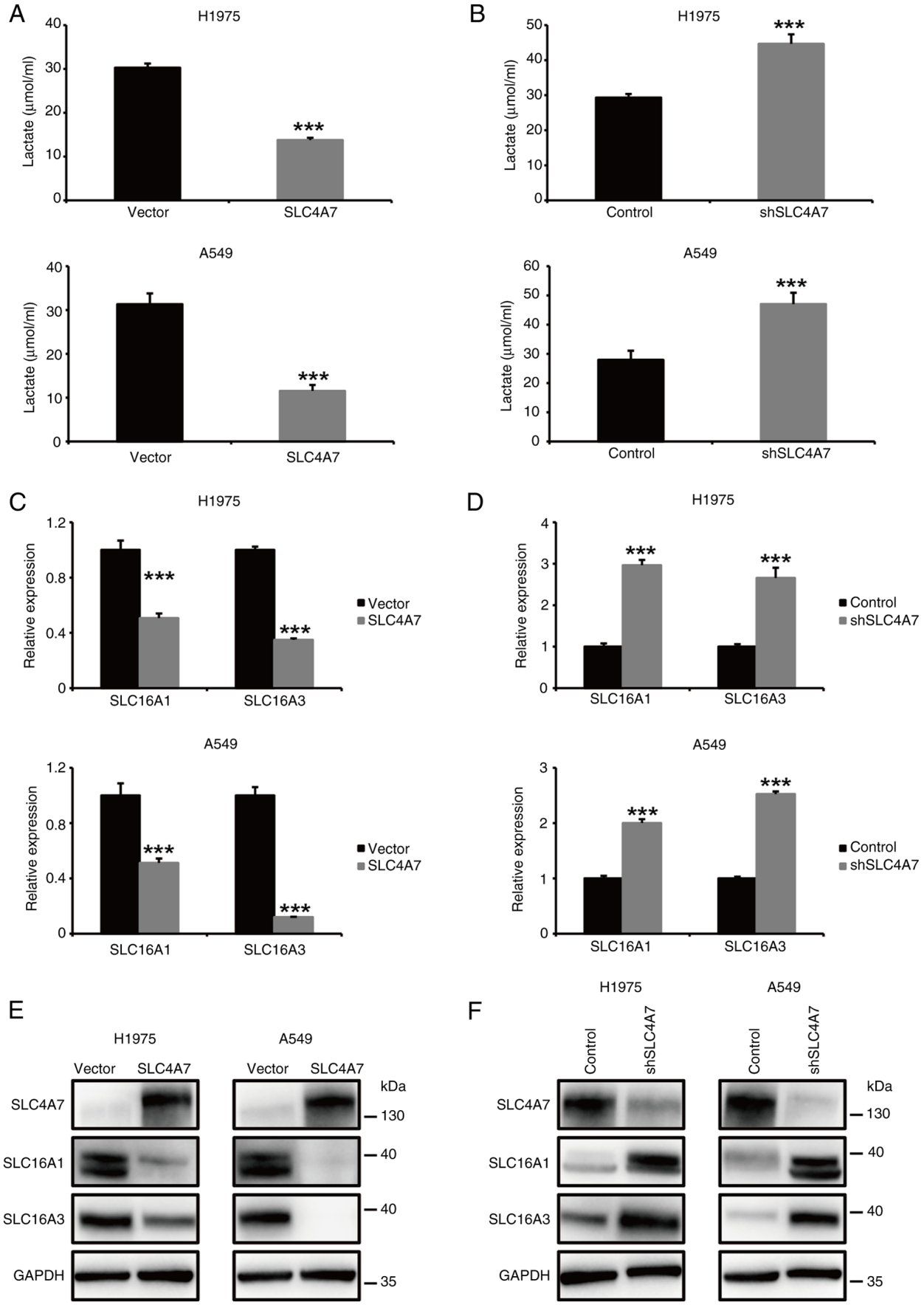

Figure 2. SLC4A7 modulates lactate transport by suppressing expression of SLC16A1/3. Extracellular lactate levels in H1975 and A549 cell lines with SLC4A7 (A) overexpression and (B) knockdown (n=6). Reverse transcription-quantitative PCR analysis of expression of SLC16A1/3 in H1975 and A549 cell lines with SLC4A7 (C) overexpression and (D) knockdown. Expression of SLC16A1/3 protein in H1975 and A549 cell lines with SLC4A7 (E) overexpression and (F) knockdown was examined by western blotting. ***P<0.001 vs. vector/control. SLC4A7, solute carrier 4A7; SLC16A1/3, solute carrier 16A1/3; sh, short hairpin.

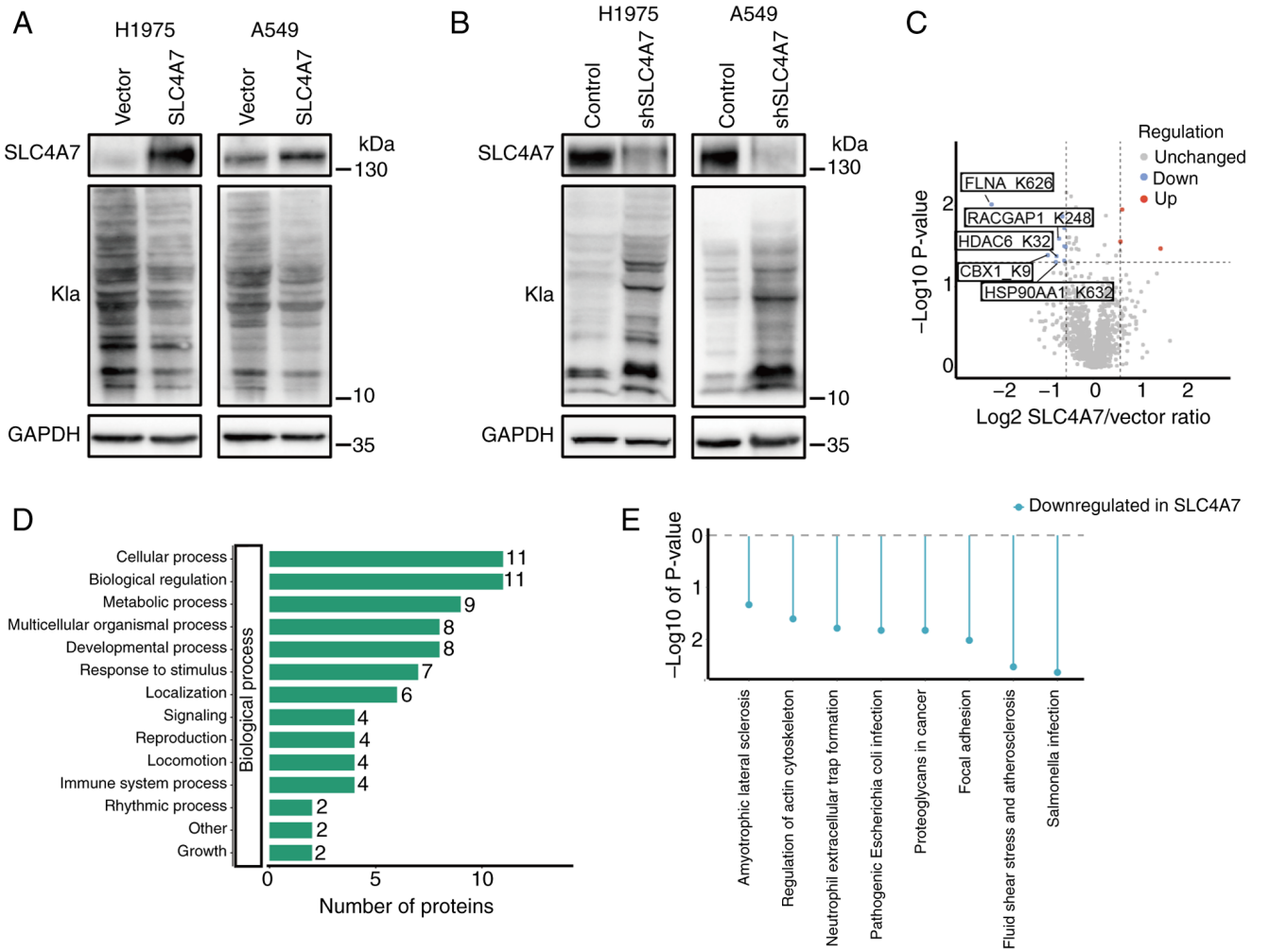

Figure 3. SLC4A7 mediates decreased protein lactylation. Western blot analysis was performed to assess lactylation of proteins in SLCA47 (A) -overexpressing and (B) -knockdown cells. (C) Differentially expressed lysine lactylation sites between SLC4A7 and vector. The cutoff values for log2 of the SLC4A7/vector ratio were set at 0.585 and -0.585, while the cutoff value for -log10 P-value was set at 1.3. Pathway enrichment analysis of lactylome data using (D) Gene Ontology and (E) Kyoto Encyclopedia of Genes and Genomes databases. SLC4A7, solute carrier 4A7; Kla, lysine lactylation.

impact of SLC4A7 on protein lactylation was investigated by western blotting using anti-pan-Kla antibody. The results demonstrated a decrease in overall protein lactylation in cell lines overexpressing SLC4A7, whereas knockdown of SLC4A7 led to enhanced protein lactylation (Fig. 3A and B). Furthermore, intracellular lactate levels were lower following SLC4A7 overexpression and increased following knockdown (Fig. S3). These findings confirmed the influence of SLC4A7 on protein lactylation. Overexpression of SLC4A7 led to decreased intracellular lactate accumulation in tumor cells.

To investigate the biological role of SLC4A7 in regulating protein lactylation, comprehensive analyses of the lactylome and proteome were conducted (Fig. S4A). Overall, 6,235 proteins (Table SI) and 2,989 Kla sites (Table SII) were identified, including quantified data for 5,294 proteins and 2,186 Kla sites (Fig. S4B and C). Comparative analysis revealed no significant difference in number of Kla sites/protein between the two groups (Fig. S4D), with >50% of the detected proteins having only one or two Kla sites (Fig. S4E). By comparing the lactylome between SLC4A7 and vector, it was observed that there were more downregulated than upregulated Kla sites associated with certain oncogenes such as HSP90AA1, HDAC6, RACGAP1, FLNA and CBX1 (46-50) (Table SIII; Fig. 3C). This confirmed that SLC4A7 could inhibit protein lactylation and impede tumor progression. The proteome dataset was subjected to the same analyses (Table SIV; Fig. S4F).

To explore the role of SLC4A7 in mediating biological processes, GO enrichment analysis was performed; SLC4A7 was primarily enriched in cellular processes related to cancer development, both in the lactylome (Fig. 3D) and proteome (Fig. S4G). KEGG enrichment analysis revealed that down-regulated proteins lactylation mediated by SLC4A7 affected various pathways, including proteoglycans and focal adhesion (Fig. 3E). These findings suggested that suppression of tumor progression by SLC4A7 may occur through numerous regulatory mechanisms.

SLC4A7 is expressed at low levels in CSCs of LUAD. Within heterogeneous tumor cell populations, only 0.05-3.00% are considered to be CSCs (51). Previous studies have identified ALDH as a potential marker of CSCs (52,53), and our previous study confirmed that ALDH$^+$ cells isolated from LUAD exhibit characteristics resembling those of CSCs, including

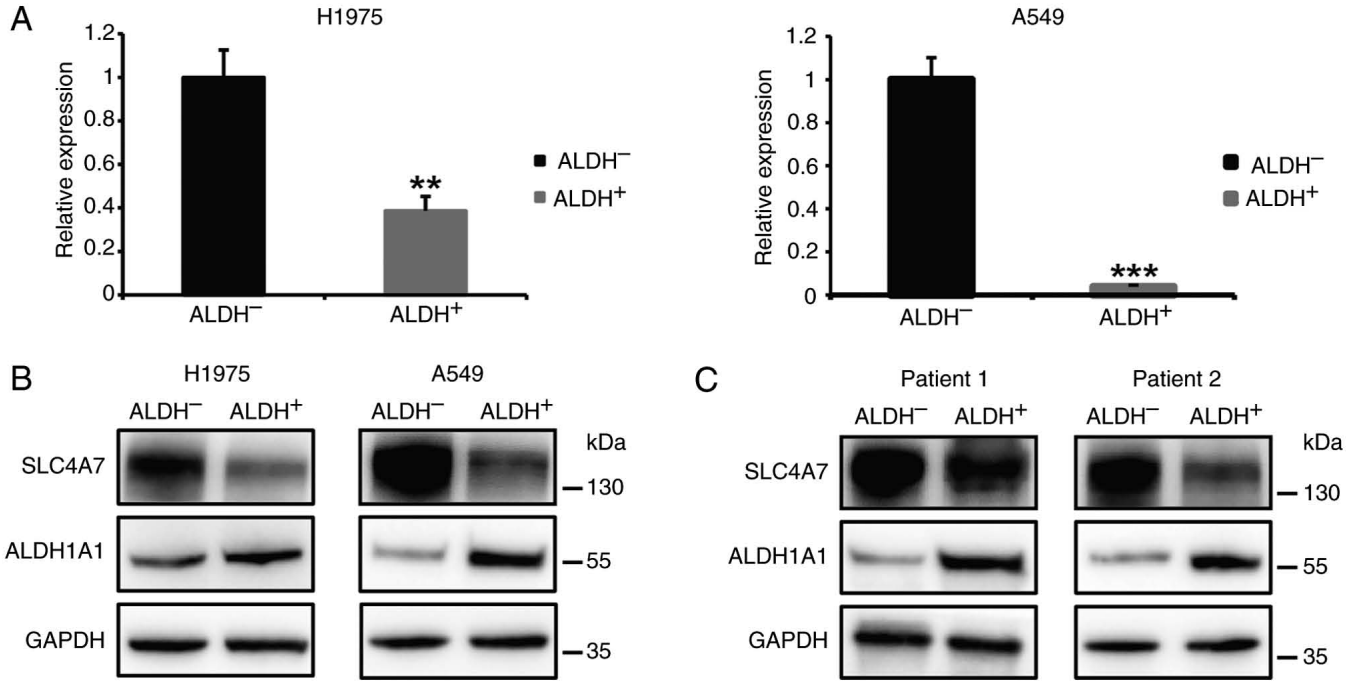

Figure 4. SLC4A7 expression is significantly downregulated in cancer stem cells of LUAD. Expression of SLC4A7 in ALDH$^{+/-}$ cells was examined by (A) reverse transcription-quantitative PCR and (B) western blotting. Each experiment was repeated three times. (C) Expression of SLC4A7 in ALDH$^{+/-}$ cells isolated from tumors of patients with LUAD was evaluated by western blotting. **P<0.01, ***P<0.001 vs. ALDH^{-}. SLC4A7, solute carrier 4A7; LUAD, lung adenocarcinoma; ALDH, aldehyde dehydrogenase.

self-renewal, increased proliferative capacity and tumorigenicity (45). The ALDH family comprises 19 isoenzymes with key physiological and toxicological functions; among them, ALDH1A1 is as the most relevant mediator of tumor stemness regulation and tumor progression (54,55). To assess the clinical relevance of SLC4A7 given the importance of CSCs in tumor initiation and progression, the association between SLC4A7 and CSCs was investigated. Our previous analysis of proteomic data revealed that SLC4A7 was significantly less expressed in CSCs of patients with LUAD compared with bulk cells (45). To confirm the expression pattern of SLC4A7 in CSCs, ALDH^{+} cells were isolated from H1975 and A549 cell lines as the CSC model while ALDH^{-} cells were used as non-CSCs. Firstly, the stem cell-like phenotypes, including stem cell marker expression, colony formation ability and proliferative capacity, were examined (Fig. S5). ALDH^{+} cells exhibited higher levels of stem cell markers such as OCT4, SOX2 and NANOG, along with increased self-renewal capacity (Fig. S5C) and stronger proliferation ability than ALDH^{-} cells (Fig. S5D), indicating resemblance to CSC properties. SLC4A7 had notably lower expression levels in ALDH^{+} compared with ALDH^{-} cells (Fig. 4A and B). This was confirmed within tumor tissue samples of patients with LUAD (Fig. 4C). Table SV shows basic patient features. Collectively, the present findings suggested that SLC4A7 may serve as a suppressor when regulating CSCs due to its low expression within LUAD.

Tumor cell stemness is suppressed by SLC4A7. To explore the role of SLC4A7 in modulating tumor cell stemness, CSC-like phenotypes were assessed by stem cell marker expression, colony formation ability and MTS assay. Overexpression of SLC4A7 significantly suppressed expression of stem cell markers (Fig. 5A and B); conversely, knockdown of SLC4A7 yielded the opposite results (Fig. 5C and D). Overexpression of SLC4A7 led to diminished colony formation capacity (Fig. 5E), while knockdown of SLC4A7 led to an increased number of colonies compared with the control (Fig. 5F). These findings suggested that SLC4A7 may restrict cellular self-renewal ability. MTS assay demonstrated a progressive decrease in cell proliferative capacity following overexpression of SLC4A7 across different cell lines (Fig. 5G), whereas knockdown of SLC4A7 resulted in enhanced cell proliferation (Fig. 5H), indicating cell proliferative potential was also regulated by SLC4A7.

Discussion

Lung cancer is the leading cause of cancer-associated mortality due to lack of effective treatment (1). Identifying more effective treatments is challenging. Recent research suggests that lactate and protein lactylation serve a critical role in tumor development (4,15) but the regulatory mechanisms of lactate and protein lactylation in cancer, particularly in lung cancer, are poorly understood.

The present findings offer novel insights into the role of SLC4A7 in suppressing LUAD progression, particularly via regulation of lactate homeostasis and CSCs. The present observations highlight the importance of SLC4A7 as a potential therapeutic target for LUAD treatment, which is urgently needed, given the lack of effective therapy and the high mortality rate associated with this disease.

Inhibition of tumor cell metastasis, invasion and proliferation mediated by SLC4A7, as evidenced by both *in vitro*

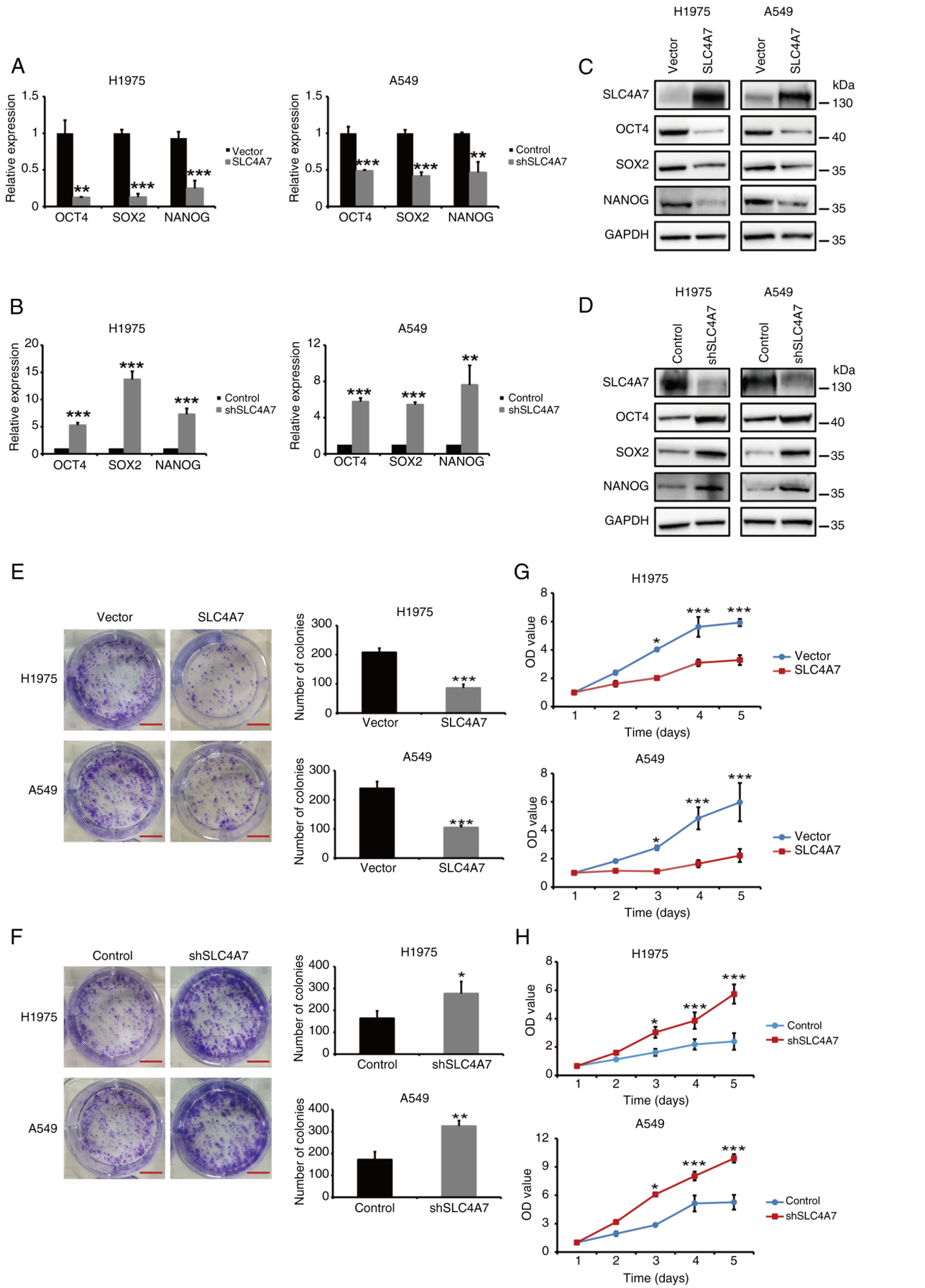

Figure 5. SLC4A7 suppresses stemness of tumor cells. The expression levels of stem cell markers were assessed using reverse transcription-quantitative PCR (A and B) and western blotting (C and D). Colony formation assay conducted in SLC4A7 (E) -overexpressing and (F) -knockdown cells. Scale bar, 1 cm. MTS assay was performed to evaluate cell viability in SLC4A7 (G) -overexpressing and (H) -knockdown cells. *P<0.05, **P<0.01, ***P<0.001. SLC4A7, solute carrier 4A7; OCT4, octamer-binding transcription factor 4; SOX2, SRY-Box Transcription Factor 2; NANOG, Nanog Homeobox.

and *in vivo* experiments, highlighted the importance of this transporter in modulating tumor behavior. The prevention of tumor formation in nude mice highlighted its potential clinical relevance. Given the absence of a successful model for lung metastasis *in vivo,* future studies should confirm the impact of SLC4A7 on tumor metastasis in an animal model. The present findings not only confirmed the inhibitory role of SLC4A7 in tumorigenesis but also suggested that it may act at an early stage to arrest tumor initiation.

The mechanism underlying the inhibitory effect of SLC4A7 on tumor progression is multifaceted, involving both extracellular and intracellular lactate regulation. The present results demonstrated that SLC4A7 significantly decreased lactate concentrations in the TME by downregulating expression of SLC16A1/3, which are key players in lactate transport. This is consistent with previous studies linking lactate accumulation to tumor aggressiveness and metastasis (1,15). By decreasing lactate levels, SLC4A7 may disrupt the lactate-fueled metabolic reprogramming that supports tumor growth and invasion.

SLC4A7 also modulated intracellular lactate levels and overall protein lactylation. The suppression of lactylation, a recently recognized post-translational modification, may have notable effects on protein function and signaling pathways involved in tumor progression. The present comprehensive analysis of the global lactylome demonstrated that SLC4A7 suppressed lactylation of numerous oncogenes and pathways, providing a potential explanation for its inhibitory effects on tumor behavior.

SLC4A7 expression was significantly lower in CSCs compared with bulk cancer cells in patients with LUAD. This, along with the inhibitory effects of SLC4A7 on CSCs-like phenotypes, suggested that SLC4A7 may serve a crucial role in regulating CSCs, which are known to drive tumor initiation, recurrence and metastasis. However, the exact mechanism by which SLC4A7 regulates lactate to inhibit CSC phenotypes remains unclear and warrants further investigation. It is possible that SLC4A7 modulates the metabolic state of CSCs, thereby altering their self-renewal and differentiation capability.

The identification of SLC4A7 as a potential tumor suppressor in LUAD provides a novel avenue for therapeutic intervention. Strategies aimed at restoring or enhancing SLC4A7 expression may be effective in inhibiting tumor growth and metastasis. Additionally, targeting lactate metabolism or lactylation may represent novel therapeutic approaches for LUAD and other malignancies.

In conclusion, the present study demonstrated that SLC4A7 inhibited LUAD progression by regulating lactate homeostasis and CSCs. These findings provide novel insights into the complex mechanisms underlying tumor development and progression and suggest potential therapeutic targets for LUAD treatment. To the best of our knowledge, the present study is the first to demonstrate the inhibitory role of SLC4A7 in regulating tumor cell stemness and mediating tumor initiation and progression. Future studies should focus on elucidating the precise regulatory mechanisms of SLC4A7, identifying its key functional domains and potential clinical applications.

Acknowledgements

Not applicable.

Funding

The present study was supported by China Postdoctoral Science Foundation (grant no. 2021M702290), Science and Technology Project of Shenzhen (grant nos. GJHZ20170310090257380 and JCYJ20170413092711058) and Shenzhen Key Laboratory of Stem Cell Research and Clinical Transformation (grant no. ZDSYS20190902093203727).

Availability of data and materials

The data generated in the present study may be found in the ProteomeXchange Consortium under accession number PXD046344 or at the following URL: proteomecentral. proteomexchange.org.

Authors' contributions

FL, JD, HY and QH designed the study. HY wrote the manuscript. HY and QH confirm the authenticity of all the raw data. HY and YG performed experiments. XH, HL, HY and LS analyzed data. All authors have read and approved the final manuscript.

Ethics approval and consent to participate

Tissues from patients diagnosed with LUAD were procured from Shenzhen People's Hospital, in accordance with the principles outlined in the Declaration of Helsinki and as approved by the Ethics Committee of Shenzhen People's Hospital (approval no. 2023-065-01). Prior to inclusion, all patients provided informed consent.

Patient consent for publication

Not applicable.

Competing interests

The authors declare that they have no competing interests.

References

1. Siegel RL, Miller KD, Wagle NS and Jemal A: Cancer statistics, 2023. CA Cancer J Clin 73: 17-48, 2023.
2. Rabinowitz JD and Enerbäck S: Lactate: The ugly duckling of energy metabolism. Nat Metab 2: 566-5671, 2020.
3. Koppenol WH, Bounds PL and Dang CV: Otto Warburg's contributions to current concepts of cancer metabolism. Nat Rev Cancer 11: 325-337, 2011.
4. Li X, Yang Y, Zhang B, Lin X, Fu X, An Y, Zou Y, Wang JX, Wang Z and Yu T: Lactate metabolism in human health and disease. Signal Transduct Target Ther 7: 305, 2022.
5. Ippolito L, Comito G, Parri M, Iozzo M, Duatti A, Virgilio F, Lorito N, Bacci M, Pardella E, Sandrini G, *et al*: Lactate rewires lipid metabolism and sustains a metabolic-epigenetic axis in prostate cancer. Cancer Res 82: 1267-1282, 2022.
6. Brown TP and Ganapathy V: Lactate/GPR81 signaling and proton motive force in cancer: Role in angiogenesis, immune escape, nutrition, and Warburg phenomenon. Pharmacol Ther 206: 107451, 2020.
7. Bergers G and Fendt SM: The metabolism of cancer cells during metastasis. Nat Rev Cancer 21: 162-180, 2021.
8. Végran F, Boidot R, Michiels C, Sonveaux P and Feron O: Lactate influx through the endothelial cell monocarboxylate transporter MCT1 supports an NF-κB/IL-8 pathway that drives tumor angiogenesis. Cancer Res 71: 2550-2560, 2011.

9. Annan DA, Maishi N, Soga T, Dawood R, Li C, Kikuchi H, Hojo T, Morimoto M, Kitamura T, Alam MT, *et al*: Carbonic anhydrase 2 (CAII) supports tumor blood endothelial cell survival under lactic acidosis in the tumor microenvironment. Cell Commun Signal 17: 169, 2019.
10. Certo M, Tsai CH, Pucino V, Ho PC and Mauro C: Lactate modulation of immune responses in inflammatory versus tumour microenvironments. Nat Rev Immunol 21: 151-161, 2021.
11. Ye L, Jiang Y and Zhang M: Crosstalk between glucose metabolism, lactate production and immune response modulation. Cytokine Growth Factor Rev 68: 81-92, 2022.
12. Fukushi A, Kim HD, Chang YC and Kim CH: Revisited metabolic control and reprogramming cancers by means of the Warburg effect in tumor cells. Int J Mol Sci 23: 10037, 2022.
13. Gnocchi D, Sabbà C and Mazzocca A: Lactic acid fermentation: A maladaptive mechanism and an evolutionary throwback boosting cancer drug resistance. Biochimie 208: 180-185, 2023.
14. Zhang D, Tang Z, Huang H, Zhou G, Cui C, Weng Y, Liu W, Kim S, Lee S, Perez-Neut M, *et al*: Metabolic regulation of gene expression by histone lactylation. Nature 574: 575-580, 2019.
15. Chen AN, Luo Y, Yang YH, Fu JT, Geng XM, Shi JP and Yang J: Lactylation, a novel metabolic reprogramming code: Current status and prospects. Front Immunol 12: 688910, 2021.
16. Jiang J, Huang D, Jiang Y, Hou J, Tian M, Li J, Sun L, Zhang Y, Zhang T, Li Z, *et al*: Lactate modulates cellular metabolism through histone lactylation-mediated gene expression in non-small cell lung cancer. Front Oncol 11: 647559, 2021.
17. Xiong J, He J, Zhu J, Pan J, Liao W, Ye H, Wang H, Song Y, Du Y, Cui B, *et al*: Lactylation-driven METTL3-mediated RNA m^6A modification promotes immunosuppression of tumor-infiltrating myeloid cells. Mol Cell 82: 1660-1677.e10, 2022.
18. Yang Z, Yan C, Ma J, Peng P, Ren X, Cai S, Shen X, Wu Y, Zhang S, Wang X, *et al*: Lactylome analysis suggests lactylation-dependent mechanisms of metabolic adaptation in hepatocellular carcinoma. Nat Metab 5: 61-79, 2023.
19. Fan M, Yang K, Wang X, Chen L, Gill PS, Ha T, Liu L, Lewis NH, Williams DL and Li C: Lactate promotes endothelial-to-mesenchymal transition via Snail1 lactylation after myocardial infarction. Sci Adv 9: eadc9465, 2023.
20. Clara JA, Monge C, Yang Y and Takebe N: Targeting signalling pathways and the immune microenvironment of cancer stem cells-a clinical update. Nat Rev Clin Oncol 17: 204-232, 2020.
21. Bayik D and Lathia JD: Cancer stem cell-immune cell crosstalk in tumour progression. Nat Rev Cancer 21: 526-536, 2021.
22. Paul R, Dorsey JF and Fan Y: Cell plasticity, senescence, and quiescence in cancer stem cells: Biological and therapeutic implications. Pharmacol Ther 231: 107985, 2022.
23. Reya T, Morrison SJ, Clarke MF and Weissman IL: Stem cells, cancer, and cancer stem cells. Nature 414: 105-111, 2001.
24. Liu S, Zhao H, Hu Y, Yan C, Mi Y, Li X, Tao D and Qin J: Lactate promotes metastasis of normoxic colorectal cancer stem cells through PGC-1α-mediated oxidative phosphorylation. Cell Death Dis 13: 651, 2022.
25. Zhao H, Yan C, Hu Y, Mu L, Liu S, Huang K, Li Q, Li X, Tao D and Qin J: Differentiated cancer cell-originated lactate promotes the self-renewal of cancer stem cells in patient-derived colorectal cancer organoids. Cancer Lett 493: 236-244, 2020.
26. Nimmakayala RK, Leon F, Rachagani S, Rauth S, Nallasamy P, Marimuthu S, Shailendra GK, Chhonker YS, Chugh S, Chirravuri R, *et al*: Metabolic programming of distinct cancer stem cells promotes metastasis of pancreatic ductal adenocarcinoma. Oncogene 40: 215-231, 2021.
27. Rives ML, Javitch JA and Wickenden AD: Potentiating SLC transporter activity: Emerging drug discovery opportunities. Biochem Pharmacol 135: 1-11, 2017.
28. Pizzagalli MD, Bensimon A and Superti-Furga G: A guide to plasma membrane solute carrier proteins. FEBS J 288: 2784-2835, 2021.
29. Lin L, Yee SW, Kim RB and Giacomini KM: SLC transporters as therapeutic targets: Emerging opportunities. Nat Rev Drug Discov 14: 543-560, 2015.
30. Marin JJG, Macias RIR, Cives-Losada C, Peleteiro-Vigil A, Herraez E and Lozano E: Plasma membrane transporters as biomarkers and molecular targets in cholangiocarcinoma. Cells 9: 498, 2020.
31. Schlessinger A, Zatorski N, Hutchinson K and Colas C: Targeting SLC transporters: Small molecules as modulators and therapeutic opportunities. Trends Biochem Sci 48: 801-814, 2023.
32. Nwosu ZC, Song MG, di Magliano MP, Lyssiotis CA and Kim SE: Nutrient transporters: Connecting cancer metabolism to therapeutic opportunities. Oncogene 42: 711-724, 2023.
33. Wang ZH, Peng WB, Zhang P, Yang XP and Zhou Q: Lactate in the tumour microenvironment: From immune modulation to therapy. EBioMedicine 73: 103627, 2021.
34. Qian Y, Galan-Cobo A, Guijarro I, Dang M, Molkentine D, Poteete A, Zhang F, Wang Q, Wang J, Parra E, *et al*: MCT4-dependent lactate secretion suppresses antitumor immunity in LKB1-deficient lung adenocarcinoma. Cancer Cell 41: 1363-1380.e7, 2023.
35. Benjamin D, Robay D, Hindupur SK, Pohlmann J, Colombi M, El-Shemerly MY, Maira SM, Moroni C, Lane HA and Hall MN: Dual inhibition of the lactate transporters MCT1 and MCT4 is synthetic lethal with metformin due to NAD+ depletion in cancer cells. Cell Rep 25: 3047-3058.e4, 2018.
36. Fang Y, Liu W, Tang Z, Ji X, Zhou Y, Song S, Tian M, Tao C, Huang R, Zhu G, *et al*: Monocarboxylate transporter 4 inhibition potentiates hepatocellular carcinoma immunotherapy through enhancing T cell infiltration and immune attack. Hepatology 77: 109-123, 2023.
37. Faubert B, Li KY, Cai L, Hensley CT, Kim J, Zacharias LG, Yang C, Do QN, Doucette S, Burguete D, *et al*: Lactate metabolism in human lung tumors. Cell 171: 358-371.e9, 2017.
38. Lee DG, Lee JH, Choi BK, Kim MJ, Kim SM, Kim KS, Chang K, Park SH, Bae YS and Kwon BS: H^+-myo-inositol transporter SLC2A13 as a potential marker for cancer stem cells in an oral squamous cell carcinoma. Curr Cancer Drug Targets 11: 966-975, 2011.
39. Yin Y, Jiang Z, Fu J, Li Y, Fang C, Yin X, Chen Y, Chen N, Li J, Ji Y, *et al*: Choline-induced SLC5A7 impairs colorectal cancer growth by stabilizing p53 protein. Cancer Lett 525: 55-66, 2022.
40. Romero MF, Chen AP, Parker MD and Boron WF: The SLC4 family of bicarbonate (HCO_3^-) transporters. Mol Aspects Med 34: 159-182, 2013.
41. Sedlyarov V, Eichner R, Girardi E, Essletzbichler P, Goldmann U, Nunes-Hasler P, Srndic I, Moskovskich A, Heinz LX, Kartnig F, *et al*: The bicarbonate transporter SLC4A7 plays a key role in macrophage phagosome acidification. Cell Host Microbe 23: 766-774.e5, 2018.
42. Boedtkjer E: Na^+,HCO_3^- cotransporter NBCn1 accelerates breast carcinogenesis. Cancer Metastasis Rev 38: 165-178, 2019.
43. Ergün S: Cross-Kingdom Gene regulation via miRNAs of Hypericum perforatum (St. John's wort) flower dietetically absorbed: An in silico approach to define potential biomarkers for prostate cancer. Comput Biol Chem 80: 16-22, 2019.
44. Shao L, He Q, Wang J, He F, Lin S, Wu L, Gao Y, Ma W, Dong J, Yang X and Li F: MicroRNA-326 attenuates immune escape and prevents metastasis in lung adenocarcinoma by targeting PD-L1 and B7-H3. Cell Death Discov 7: 145, 2021.
45. Luo HT, Zheng YY, Tang J, Shao LJ, Mao YH, Yang W, Yang XF, Li Y, Tian RJ and Li FR: Dissecting the multi-omics atlas of the exosomes released by human lung adenocarcinoma stem-like cells. NPJ Genom Med 6: 48, 2021.
46. Niu M, Zhang B, Li L, Su Z, Pu W, Zhao C, Wei L, Lian P, Lu R, Wang R, *et al*: Targeting HSP90 inhibits proliferation and induces apoptosis through AKT1/ERK pathway in lung cancer. Front Pharmacol 12: 724192, 2022.
47. Hu C, Zhang M, Moses N, Hu CL, Polin L, Chen W, Jang H, Heyza J, Malysa A, Caruso JA, *et al*: The USP10-HDAC6 axis confers cisplatin resistance in non-small cell lung cancer lacking wild-type p53. Cell Death Dis 11: 328, 2020.
48. Wu PH, Onodera Y, Recuenco FC, Giaccia AJ, Le QT, Shimizu S, Shirato H and Nam JM: Lambda-carrageenan enhances the effects of radiation therapy in cancer treatment by suppressing cancer cell invasion and metastasis through Racgap1 inhibition. Cancers (Basel) 11: 1192, 2019.
49. Nallapalli RK, Ibrahim MX, Zhou AX, Bandaru S, Sunkara SN, Redfors B, Pazooki D, Zhang Y, Borén J, Cao Y, *et al*: Targeting filamin A reduces K-RAS-induced lung adenocarcinomas and endothelial response to tumor growth in mice. Mol Cancer 11: 50, 2012.
50. Reyes-Castro RA, Chen SY, Seemann J, Kundu ST, Gibbons DL and Arur S: Phosphorylated nuclear DICER1 promotes open chromatin state and lineage plasticity of AT2 tumor cells in lung adenocarcinomas. Sci Adv 9: eadf6210, 2023.
51. Han J, Won M, Kim JH, Jung E, Min K, Jangili P and Kim JS: Cancer stem cell-targeted bio-imaging and chemotherapeutic perspective. Chem Soc Rev 49: 7856-7878, 2020.

52. Toledo-Guzmán ME, Hernández MI, Gómez-Gallegos ÁA and Ortiz-Sánchez E: ALDH as a stem cell marker in solid tumors. Curr Stem Cell Res Ther 14: 375-388, 2019.
53. Ginestier C, Hur MH, Charafe-Jauffret E, Monville F, Dutcher J, Brown M, Jacquemier J, Viens P, Kleer CG, Liu S, *et al*: ALDH1 is a marker of normal and malignant human mammary stem cells and a predictor of poor clinical outcome. Cell Stem Cell 1: 555-567, 2007.
54. Liu C, Qiang J, Deng Q, Xia J, Deng L, Zhou L, Wang D, He X, Liu Y, Zhao B, *et al*: ALDH1A1 activity in tumor-initiating cells remodels myeloid-derived suppressor cells to promote breast cancer progression. Cancer Res 81: 5919-5934, 2021.
55. Ge X, Li M, Song GX, Zhang Z, Yin J, Ge Z, Shi Z, Liu LZ, Jiang BH, Qian X and Shen H: Chromium (VI)-induced ALDH1A1/EGF axis promotes lung cancer progression. Clin Transl Med 12: e1136, 2022.